J Solid State Electrochem (2010) 14:1829–1834
DOI 10.1007/s10008-009-1001-4

ORIGINAL PAPER

Silicon nanowires with and without carbon coating as anode materials for lithium-ion batteries

Huixin Chen · Zhixin Dong · Yanpeng Fu · Yong Yang

Received: 17 November 2009 / Revised: 23 December 2009 / Accepted: 31 December 2009 / Published online: 28 January 2010

Abstract Silicon nanowires (Si NWs) with and without carbon coating were successfully prepared by combination of chemical vapor deposition and thermal evaporation method. The morphologies, structures, and compositions of these nanomaterials were characterized in detail. Furthermore, the electrochemical performances of uncoated and carbon-coated Si NWs as anode materials were also studied. It shows that the carbon-coated Si NWs electrode has higher capacity, better cycle stability, and rate capability than the uncoated materials. For example, it delivers 3,702 and 3,082 mAh g^{-1} in the initial charge and discharge processes. When cycled between 0.02 and 2.0 V at a current density of 210 mA g^{-1}, it yields a high coulombic efficiency of 83.2%. The discharge capacity still remains around 2,150 mAh g^{-1} after 30 cycles.

Keywords Si NWs · Electrochemical performance · Lithium-ion batteries · Carbon-coated

Introduction

The development of a new generation of lithium-ion batteries requires new anode materials with high energy capacity and long cycle life for applications in portable electronic devices, electric vehicles, and implantable medical devices [1]. In contrast to the anode materials such as Al, Sn, and Si which can make alloys with lithium, silicon is an attractive anode material for lithium batteries due to its high theoretical specific capacity (4,200 mAh g^{-1}) and abundant sources [2–4]. However, due to its volume swell by 400% upon lithium insertion and extraction, which results in pulverization and fast capacity fading of the material [5], silicon has not been developed into a commercial product yet. In recent years, Si nanomaterials are studied as a new class of anode materials for lithium-ion batteries to replace carbon-based materials [6–13] in practical use. For example, Cui et al. [6] prepared Si nanowires (Si NWs) by directly growing on the current collector and the product does not pulverize or break into smaller particles after cycling. They believed that facile strain relaxation in the nanowires allowed them to increase in diameter and length without breaking of the wires. Moreover, in their design, the Si NWs were connected tightly with the current collector, allowing for efficient 1D electron transport down the length of every nanowire [6, 7]. However, a low initial coulombic efficiency of 73% was observed in their product, indicating a poor reversibility [6]. Groner et al. reported that electron migrations can be somewhat faster by the tunneling effect when the pore size of coating layer is less than several nanometers [14]. Yoshio et al. [15–17] employed carbon coating to prepare silicon-based composite under various conditions. The carbon-coated silicon showed superior cyclic performance compared with the conventional silicon.

For improving the low initial coulombic efficiency and obtaining the superior cyclic performance, silicon maybe developed into a commercial product. In this work, we prepared Si NWs and carbon-coated Si NWs electrodes by chemical vapor deposition method and evaporation method. The electrochemical performances of uncoated and carbon-coated Si NWs as anode materials were also studied.

H. Chen · Z. Dong · Y. Fu · Y. Yang (✉)
State Key Laboratory for Physical Chemistry of Solid Surfaces,
College of Chemistry and Chemical Engineering,
Department of Chemistry, Xiamen University,
Xiamen 361005 Fujian, People's Republic of China
e-mail: yyang@xmu.edu.cn

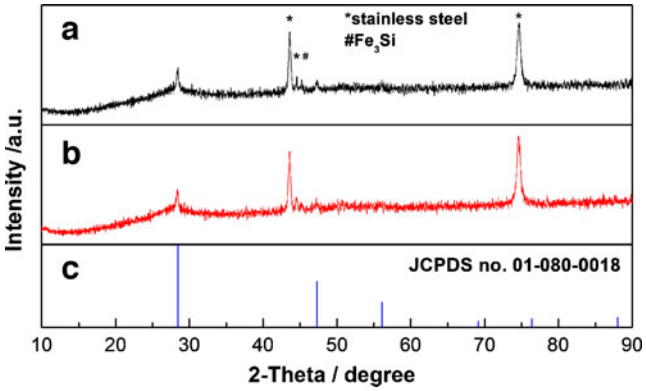

Fig. 1 XRD patterns of **a** carbon-coated Si NWs, **b** pristine Si NWs, and **c** silicon standard

Experimental details

Si NWs were grown via a vapor–liquid–solid (VLS) growth method, i.e., a stainless steel 304 (0.5 mm thick) substrate was decorated with a 10-nm-thick Au catalyst film by using e-beam evaporation. The substrate was then transferred into a chemical vapor deposition tube furnace. The gold thin film was annealed at 600 °C for 2 h under H_2 flow, and subsequently, Si NWs were grown at 540 °C with SiH_4/H_2 mixed gas as the precursor. The carbon-coated Si NWs was obtained by carbon evaporation on the surface of the Si NWs. The masses of the Si NWs (~1 mg) and carbon (~50 μg) were measured on a microbalance (Mettler Toledo XS3DU, 1 μg resolution). X-ray diffraction (XRD) patterns of the samples were obtained on a PANalytical X'Pert with Cu K_α radiation. Structure and morphology characterization were carried out on scanning electron microscopy (SEM; Hitachi S4800) with a high sensitivity energy-dispersive X-ray spectrometer (EDS) and transmission electron microscopy (TEM; Philips Tecnai F30, acceleration voltage 300 kV). A 300-kV Hitachi HD-2300A scanning transmission electron microscope (STEM) was used to do a chemical content analysis. The cells (CR2025 coin type) were assembled in an argon-filled glove box (MBraun Labmaster 130) where both moisture and oxygen levels were kept at <1 ppm. The electrolyte used was 1 mol/L $LiPF_6$ in ethylene carbonate and dimethyl carbonate (1:1, *v*/*v*) and lithium foil was used as the counter electrode. The galvanostatic charge–discharge were carried out on a Land CT2001A cell test system with a voltage range of 0.02–2.0 V (versus Li/Li^+) at room temperature. Cyclic voltammetry (CV) was performed on CHI608A, scanned from 2.0 to 0.01 V versus Li/Li^+ at a scan rate of 0.5 mV s^{-1}.

Results and discussion

Structure and morphology

Figure 1 shows the XRD patterns of carbon-coated Si NWs, pristine Si NWs, and single-crystalline silicon pellet. To make sure that Si NW was coated, we compared the XRD patterns of the Si NWs with and without carbon coating. The XRD patterns of the pristine Si NWs and carbon-coated Si NWs are similar, and both can be ascribed to the existence of Si, α-$FeSi_2$, and stainless steel. No obvious shift in 2θ position or phase impurities was observed after coating process. The absence of diffraction peaks from carbon may be due to its low content and amorphous structure. The α-$FeSi_2$ was formed at the interface between the stainless steel and the Si wires at high temperature (540 °C) [17].

Figure 2a shows a typical SEM image of the uncoated Si NWs grown on a stainless steel substrate. A large quantity of nanowires was obtained on the substrate. The EDS analysis (inset) proves that the nanowires are composed of Si with trace of oxygen, which was attributed to the surface oxidation products sheathing on the nanowires. Au as catalyst was also observed. The SEM image shown in Fig. 2b reveals that the Si NW has a diameter of about

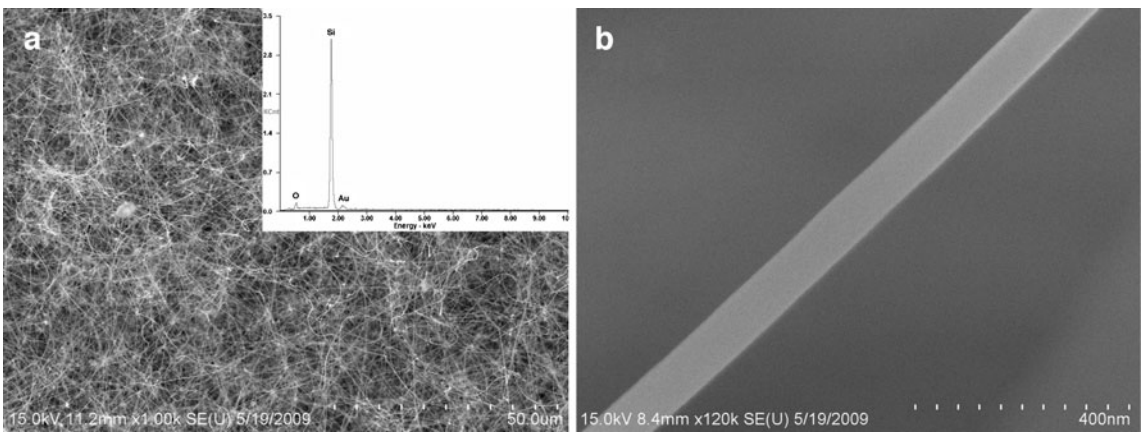

Fig. 2 **a** SEM image of the Si NWs without carbon coating. The *inset* shows the corresponding EDS analysis. **b** SEM image of an individual Si NW without carbon coating

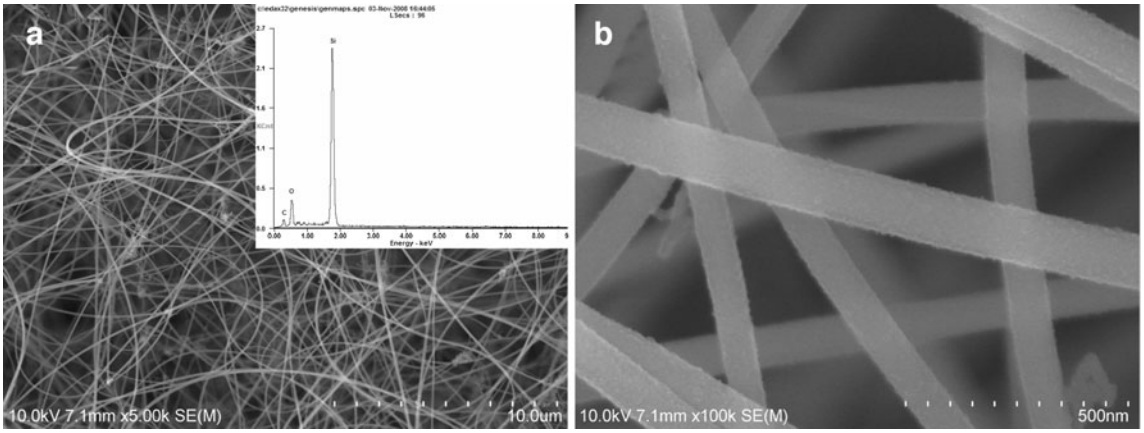

Fig. 3 **a** SEM image of the Si NWs with carbon coating. The *inset* shows the corresponding EDS analysis. **b** SEM image of an individual Si NW with carbon coating

90 nm, and the surface is fairly smooth. Figure 3a shows the image of carbon-coated Si NWs; no difference was observed compared to that of the uncoated one (Fig. 2a). The corresponding EDS analysis (inset) demonstrates that the carbon-coated Si NWs are composed of Si, silicon oxidation, and carbon. On a magnified observation, we can find that the surface of the carbon-coated Si NW is quite rough.

Figure 4 shows the TEM image of the carbon-coated Si NW. A compact coating layer is clearly observed on the surface of the Si NW. Si NWs produced by the VLS method show excellent crystallinity, although the surfaces may be coated by a thick surface oxide layer [15]. Cui et al. also proved that Si NWs grown with silane reactant in hydrogen are single crystals with little or no visible amorphous oxide down to diameters as small as 3 nm [19]. Therefore, we believe that the coating layer observed in our carbon-coated sample may consist of carbon and silicon oxide. Accordingly, further investigation was carried out by STEM. The STEM image of an individual carbon-coated Si NW was shown in Fig. 5a, and the corresponding line-scanning elemental analysis (Fig. 5b) was done along the line marked as mn in Fig. 5a. The content evolutions of Si and C are apparent in Fig. 5b. Nearing the starting point m (the position of 0 nm in Fig. 5b), since the electron beam had not reached the surface of the Si NWs, the amount of the Si and C were pretty low. The content of C increased rapidly at 10 nm but the huge jump of the content of Si did not show up until 20 nm which gives us the strong evidence that a 10-nm carbon layer had formed on the surface of the Si NWs.

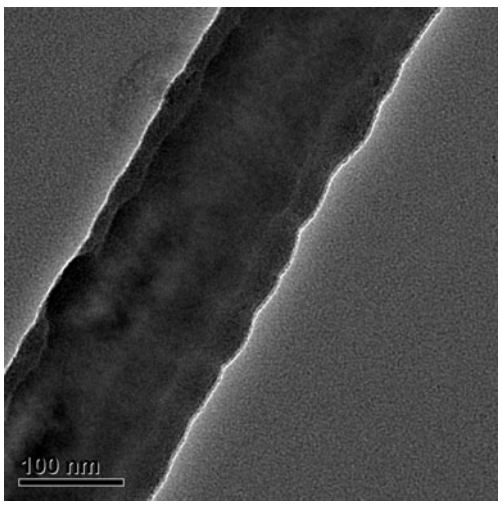

Fig. 4 TEM images of carbon-coated Si NWs

Electrochemical performance

Initial charge–discharge performance

The initial charge and discharge curves for the Si NWs with and without carbon coating between 0.02 and 2.0 V at a current density of 210 mA g^{-1} are shown in Fig. 6. The initial discharge capacity of the Si NWs without carbon coating material is 3,125.1 mAh g^{-1}, while the charge capacity is only 2,170.8 mAh g^{-1}, indicating a low coulombic efficiency of 69.5%. The initial discharge capacity of the carbon-coated Si NWs increases to 3,701.8 mAh g^{-1}, and the charge capacity increases to 3,081.6 mAh g^{-1}, giving a coulombic efficiency of 83.2%. Obviously, the carbon-coated Si NWs material delivers much higher charge–discharge capacity than that of the Si NWs without carbon coating. Moreover, the coulombic efficiency increases from 69.5% to 83.2%. Here, we believe that the presence of the carbon layer could result in the increase of the electronic conductivity and suppress the reductive decomposition of the electrolyte solution on the surface. Cyclic voltammetric results will provide further evidence to support this conclusion as shown in the following discussion.

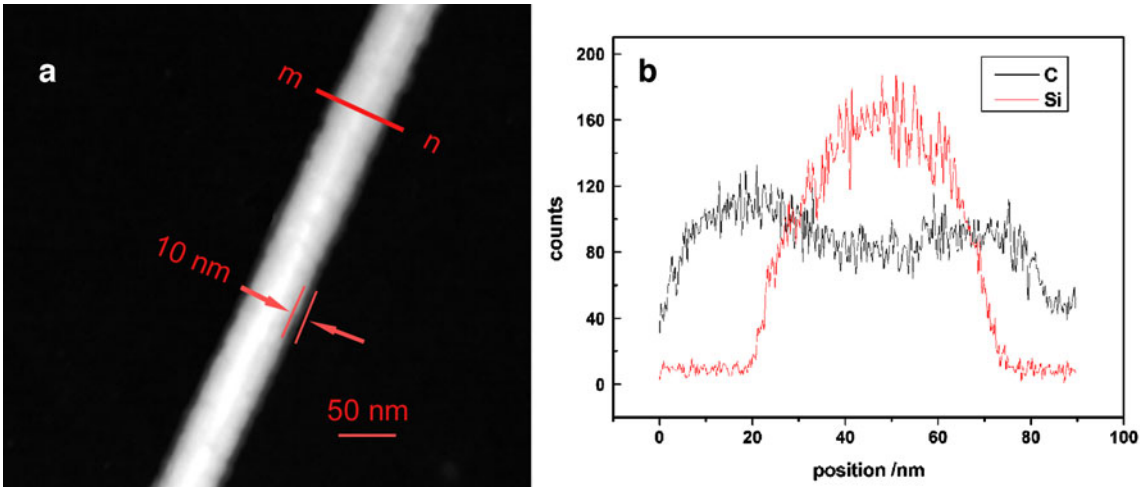

Fig. 5 **a** STEM image and **b** line-scanning elemental map of an individual carbon-coated Si NW

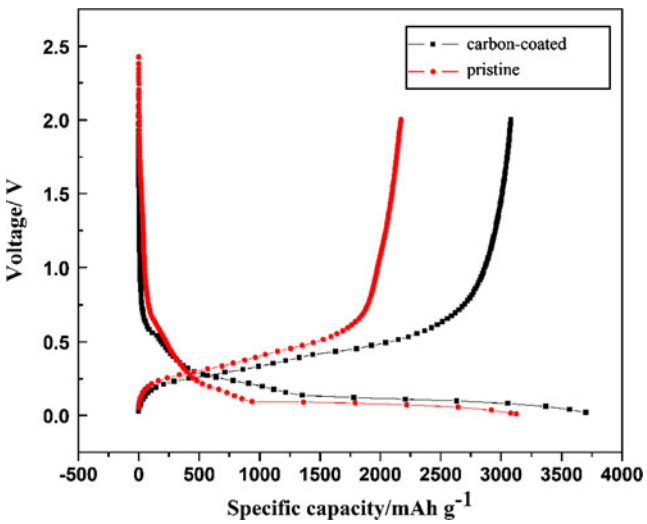

Fig. 6 Initial charge–discharge curves of the Si NWs with and without carbon coating at 0.05 C rate

Cycling performance of the materials

Figure 7 shows the capacity and coulombic efficiency as a function of cycle number for Si NWs with and without carbon coating at 0.05 C (1 C=4,200 mAh g^{-1}) rate. The capacity of the Si NWs without carbon coating decreases gradually during charge–discharge cycling and it drops to 1,992.1 mAh g^{-1} (63.7% of its initial discharge capacity) after 15 cycles. However, the capacity retention ratio of the carbon-coated Si NWs increases to 75% after 15 cycles at 0.05 C. Moreover, the coulombic efficiency of the carbon-coated materials maintains above 95% after the initial cycle, revealing a good reversibility of the electrochemical reactions. Fey et al. reported that TiO_2 coating could enhance cyclability of $LiCoO_2$ cathodes, the result was attributed to a suppression of the reaction between the cathode surface and the electrolyte and an optimization of the solid electrolyte interphase (SEI) layer [21, 22]. Apparently, the presence of our carbon layer benefits the

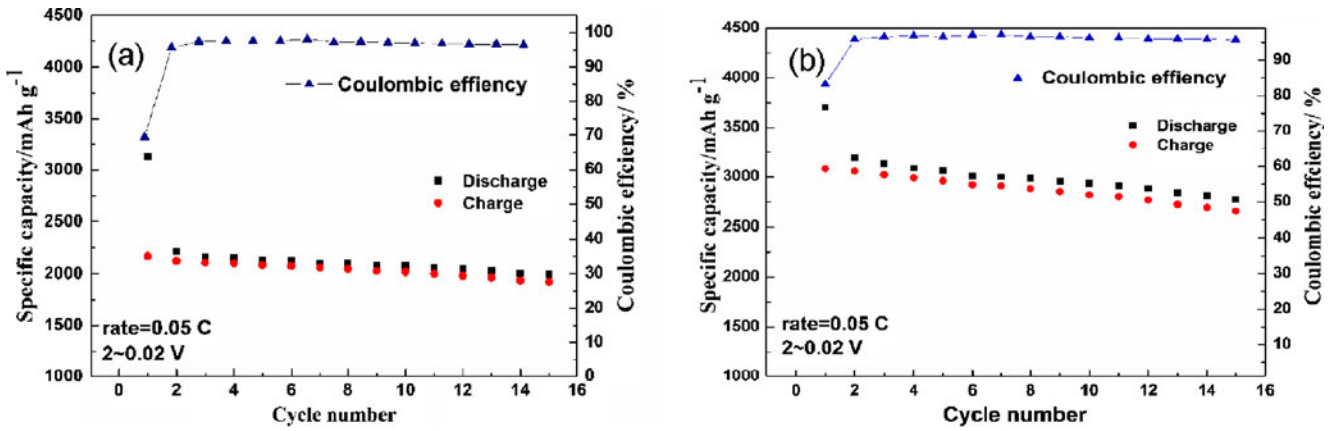

Fig. 7 Capacity and coulombic efficiency as a function of cycle number for Si NWs with (**b**) and without (**a**) carbon at 0.05 C rate

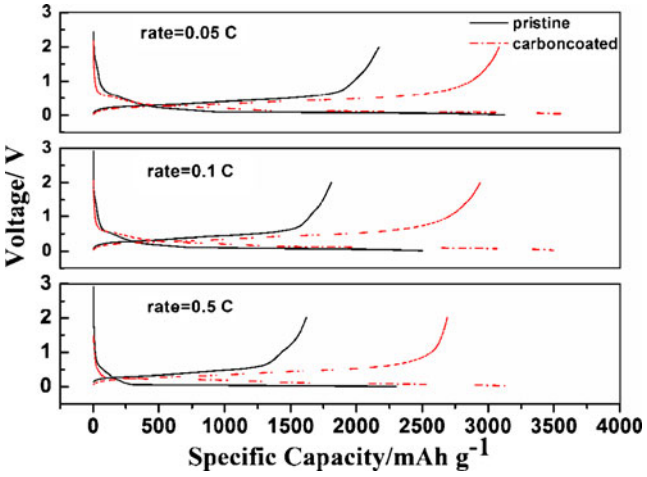

Fig. 8 Initial charge–discharge curves for the Si NWs with and without carbon coating at 0.05, 0.1, and 0.5 C rate

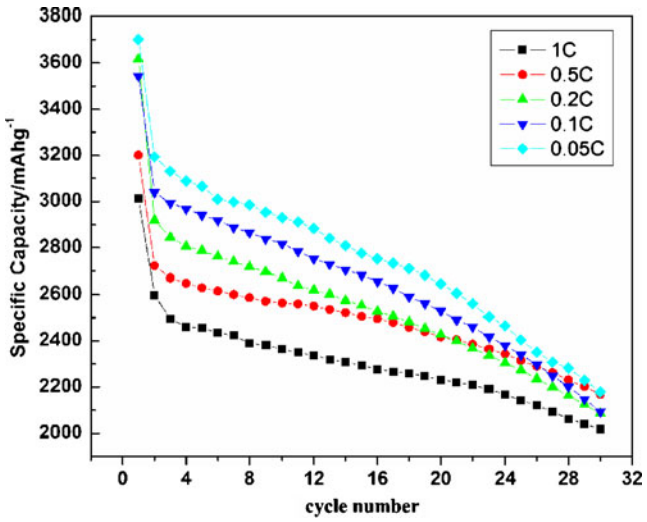

Fig. 9 Capacity–cycle number curves for Si NWs with carbon coating at 0.05, 0.1, 0.2, 0.5, and 1 C rate

cyclic stability and charge–discharge efficiency of the carbon-coated Si NWs.

Rate capability

Figure 8 shows the charge–discharge curves at different rates for 0.05, 0.1, and 0.5 C. We can see that all the carbon-coated Si NWs have higher capacity than the uncoated ones at different rates. The discharge capacities are 3,701.8 mAh g^{-1}at 0.05 C and 3,542.5 mAh g^{-1}at 0.1 C for the coated one. Even at relatively high rate of 0.5 C, the carbon-coated Si NWs can still deliver an excellent capacity of over 3,200.6 mAh g^{-1} which shows that our materials have really good charge–discharge performances. We also investigated the cycling performances of the carbon-coated Si NWs material at various current densities as presented in Fig. 9. The discharge capacity retention ratios are about 60% of its initial capacity after 30 cycles at all different currents. It is also been proved that the carbon-coated Si NWs material shows a better cycling performance at various currents compared to the uncoated one.

Cyclic voltammetry

CV curves of the Si NWs in the initial seven cycles with and without carbon coating between 0.01 and 2.0 V at a scan rate of 0.5 mV s^{-1} are shown in Fig. 10. Figure 10a shows the CV of the Si NWs without carbon coating. From the results, a discharge current peak associated with the formation of the Li–Si alloy began at a potential of about 330 mV and became quite large below 100 mV. In the charging process, current peaks appeared at about 370 and 510 mV. The current peak that appeared in the voltage range of 0.5–0.7 V may due to the formation process of SEI

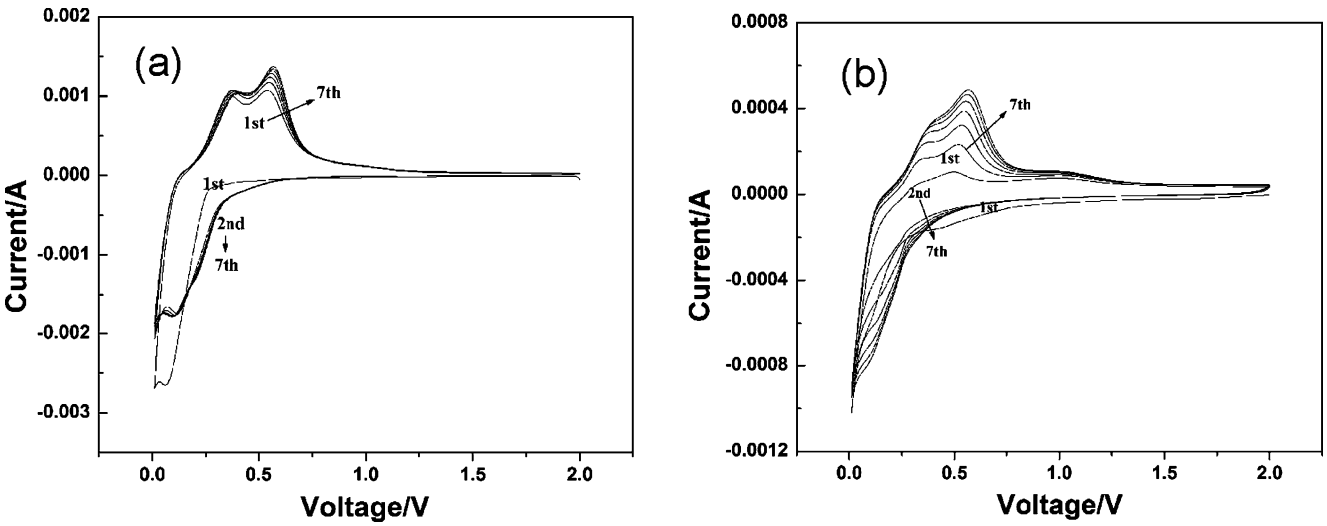

Fig. 10 CV of the Si NWs with (**b**) and without (**a**) carbon coating between 0.01 and 2.0 V at a scan rate of 0.5 mV s^{-1} versus Li/Li+

layer [6]. The increasing magnitude of the current peaks in cycling may be due to the gradual electrochemical activation of the electrode in scan. The small peak at 150–180 mV may have been caused by the reaction between Li and gold catalyst, which makes a negligible contribution to the charge capacity [6]. As a comparison, there are no apparent current peaks relating to SEI layer formation in the voltage range in the first charge of carbon-coated Si NWs material. Although the formation of the SEI of the silicon material may occur in the later long cycles, the relative capacity loss contributing to the initial irreversible capacity in the first cycle would be smaller than Si NWs without carbon coating. It supports our assumption that the carbon layer can increase the electronic conductivity and suppress the reductive decomposition of the electrolyte solution on the surface.

Conclusion

Carbon-coated Si NWs electrodes were successfully synthesized with chemical vapor deposition and evaporation method. The diameter of the Si NW is about 90 nm with an 10-nm carbon-coated layer. Compared with the Si NWs without carbon coating, discharge capacity, cycle performance, and rate capability of the carbon-coated Si NWs have been improved significantly. It delivers 3,701.8 and 3,081.6 mAh g^{-1} for the first charge–discharge capacity when cycled between 0.02 and 2.0 V with the current rate of 0.05 C, indicating a coulombic efficiency of 83.2%. The capacity still remains above 2,150 mAh g^{-1} after 30 cycles. It was also proved that the carbon-coated Si NWs material had a good cycling performance at various current densities.

The presence of the carbon layer could improve the electrochemical performances of the Si NWs, resulting to the increase of the electronic conductivity and suppression of the reductive decomposition of the electrolyte solution on the surface. Moreover, because the conductive property of carbon is better than silicon, the distribution of the electric field becomes more uniform, depressing the cross-potential aroused by polarization.

Acknowledgments This work was financially supported by National Natural Science Foundation of China (no. 90606015) and the National Basic Research Program of China (973 program, grant no. 2007CB209702).

References

1. Nazri GA, Pistoia G (2004) Lithium batteries: science and technology. Kluwer Academic, Boston
2. Moffat WG (1990) In: Moffatt WG (ed) The handbook of binary phase diagrams. Genium, New York
3. Besenhard JO (1999) In: Besenhard T (ed) Handbook of battery materials. Wiley-VCH, Weiheim, pp 363–380
4. Weydanz WJ, Wohlfahrt-Mehrens M, Huggins RA (1999) J Power Sources 81–82:237–242
5. Boukamp BA, Lesh GC, Huggins RA (1981) J Electrochem Soc 128:725–729
6. Chan CK, Peng HL, Liu G, McIlwrath K, Zhang XF, Huggins RA, Cui Y (2008) Nat Nanotechnol 3(1):31–35
7. Laik B, Eude L, Pereira-Ramos JP, Cojocaru CS, Pribat D, Rouviere E (2008) Electrochim Acta 53(17):5528–5532
8. Cui LF, Ruffo R, Chan CK, Peng HL, Cui Y (2009) Nano Lett 9 (1):491–495
9. Graetz J, Ahn CC, Yazami R, Fultz B (2003) Electrochem Solid-State Lett 6(9):A194–A197
10. Li C, Gu C, Liu Z T, Mi J X, Yang Y (2005) Chem Phys Lett 411:198–202
11. Li C, Liu Z T, Gu C, Xu X, Yang Y (2006) Adv Mater 18:228-234
12. Liu Z T, Fu Y P, Li C, Yang Y (2006) Electrochemistry (Chinese) 12(4):363-367
13. Fu Y P; Chen H X; Yang Y (2009) Electrochemistry (Chinese) 15 (1):56-61
14. Groner MD, Elam JW, Fabreguette FH, George SM (2002) Thin Solid Films 413:186–197
15. Dimov N, Kugino S, Yoshio M (2003) Electrochim Acta 48:1579–1587
16. Umeno T, Fukuda K, Wang H, Dimov N, Iwao T, Yoshio M (2001) Chem Lett 30:1186–1187
17. Dimov N, Fukuda K, Umeno T, Kugino S, Yoshio M (2003) J Power Sources 114:88–95
18. Netz A, Huggins RA, Weppner W (2003) J Power Sources 119–121:95–100
19. Wang N, Tang YH, Zhang YF, Lee CS, Bello I, Lee ST (1999) Chem Phys Lett 299:237–242
20. Wu Y, Cui Y, Huynh L, Barrelet CJ, Bell DC, Lieber CM (2004) Nano Lett 4(3):433–436
21. Fey GTK, Lu CZ, Kumar TP, Chang YC (2005) Surf Coat Technol 199:22–31
22. Fey GTK, Lu CZ, Huang JD, Kumar TP, Chang YC (2005) J Power Sources 146:65–70